



CrossMark  
click for updates

Cite this: *J. Mater. Chem. A*, 2014, 2, 18547

# Piezoelectric nanogenerators synthesized using KNbO<sub>3</sub> nanowires with various crystal structures†

Mi-Ri Joung,<sup>a</sup> Haibo Xu,<sup>a</sup> In-Tae Seo,<sup>a</sup> Dae-Hyeon Kim,<sup>a</sup> Joon Hur,<sup>b</sup> Sahn Nahm,<sup>\*abc</sup> Chong-Yun Kang,<sup>bc</sup> Seok-Jin Yoon<sup>c</sup> and Hyun-Min Park<sup>d</sup>

KNbO<sub>3</sub> (KN) nanowires having a tetragonal structure or a polymorphic phase boundary (PPB) structure, which contains both tetragonal (*P4mm*) and orthorhombic (*Amm2*) structures, are formed at low temperatures. The presence of tetragonal and PPB KN nanowires is attributed to the existence of OH<sup>−</sup> and H<sub>2</sub>O defects. Further, the tetragonal and PPB KN nanowires change to orthorhombic KN nanowires in the temperature range between 300 and 400 °C owing to desorption of the lattice hydroxyl group. A composite consisting of polydimethylsiloxane (PDMS) and KN nanowires having a PPB structure shows large dielectric constant and low dielectric loss values of 9.2 and 0.5%, respectively, at 100 kHz. Moreover, a nanogenerator (NG) synthesized using the PPB KN nanowires exhibits the largest output voltage and current among NGs synthesized using the tetragonal or orthorhombic KN nanowires. In particular, the NG containing 0.7 g of PPB KN nanowires shows an output voltage of 10.5 V and an output current of 1.3 μA; these values are among the highest ever reported for NGs synthesized using a lead-free composite. In addition, this NG exhibited the maximum output power and energy conversion efficiency, which were 4.5 μW and 0.9%, respectively, for an external load of 1.0 MΩ.

Received 11th July 2014  
Accepted 9th September 2014

DOI: 10.1039/c4ta03551h

www.rsc.org/MaterialsA

## Introduction

Piezoelectric nanogenerators (NGs) have attracted significant attention because they can convert wasted mechanical energy into electrical energy, which can be used to power nano-devices.<sup>1–10</sup> ZnO nanowires have been most frequently used for the synthesis of piezoelectric NGs; in particular, NGs synthesized using ZnO thin films have been reported to generate a high output energy density of 0.88 W cm<sup>−3</sup>.<sup>3</sup> However, the piezoelectric strain constant (*d*<sub>33</sub>) of ZnO is approximately 12 pC N<sup>−1</sup>,<sup>6,11</sup> which is much smaller than those of piezoelectric materials such as Pb(Zr,Ti)O<sub>3</sub> (PZT), BaTiO<sub>3</sub> (BT), and (Na<sub>1−x</sub>K<sub>x</sub>)NbO<sub>3</sub> (NKN). Therefore, a higher electrical energy output is expected from NGs synthesized using piezoelectric materials with high *d*<sub>*ij*</sub> values because the output energy density produced by a piezoelectric NG is proportional to *d*<sub>*ij*</sub><sup>2</sup>.<sup>12–14</sup>

In general, PZT-based materials show the highest *d*<sub>33</sub> values. Indeed, NGs synthesized using a composite of polydimethylsiloxane (PDMS) and Pb(Mg<sub>1/3</sub>Nb<sub>2/3</sub>)–PbTiO<sub>3</sub> nanowires having a high *d*<sub>33</sub> value of 371 pm V<sup>−1</sup> produced high output voltages of up to 7.8 V and high output currents of up to 2.29 μA.<sup>8</sup> However, since PZT nanowires contain 60 wt% PbO, they can cause environmental problems; moreover, they cannot be used for the fabrication of biomedical devices. NGs synthesized using BT nanoparticles and BT nanotubes exhibited promising output voltages (3.2–5.5 V) and output currents (~350 nA).<sup>4,6</sup> However, the Curie temperature (*T*<sub>c</sub>) of BT is low (~120 °C); therefore, it cannot be used for the fabrication of devices working at high temperatures.<sup>15</sup> NGs consisting of a composite of NaNbO<sub>3</sub> nanowires and PDMS were also investigated, but their output voltage (3.2 V) and output current (72 nA) were relatively small because the NaNbO<sub>3</sub> ceramic has a small *d*<sub>33</sub> value of 50 pC N<sup>−1</sup>.<sup>7,16</sup> On the other hand, NGs synthesized using a composite of 0.942 (K<sub>0.48</sub>Na<sub>0.535</sub>)NbO<sub>3</sub>–0.058LiNbO<sub>3</sub> (KNLN) nanoparticles, Cu nanorods, and PDMS showed a high output voltage of 12 V and a high output current of 1.2 μA because the KNLN ceramic has a large *d*<sub>33</sub> value of 310 pC N<sup>−1</sup>.<sup>9</sup>

The KNbO<sub>3</sub> (KN) ceramic has been considered as a good candidate for lead-free piezoelectric ceramics because a KN single crystal exhibits good piezoelectric properties and high *T*<sub>c</sub>.<sup>17,18</sup> Therefore, KN nanowires and nanoparticles have been synthesized for various applications, and their structural and electrical properties have been investigated.<sup>5,19–24</sup> Moreover, NGs were synthesized using KN nanowires and PDMS (K–P)

<sup>a</sup>Department of Materials Science and Engineering, Korea University, 1-5 Ga, Anam-dong, Seongbuk-gu, Seoul 136-701, Korea. E-mail: snahm@korea.ac.kr; Fax: +82 2 928 3584; Tel: +82 2 3290 3279

<sup>b</sup>Department of Information Technology-Nano Science, Korea University-Korea Institute of Science and Technology School, Korea University, 1-5 Ga, Anam-dong, Seongbuk-gu, Seoul 136-713, Republic of Korea

<sup>c</sup>Electronic Materials Center, Korea Institute of Science and Technology, 39-1 Hawolkok-dong, Seongbuk-gu, Seoul, 137-791, Republic of Korea

<sup>d</sup>Center for Nanomaterials Characterization, Korea Research Institute of Standards and Science, 267 Gajeong-ro, Yuseong-gu, Daejeon 305-340, Republic of Korea

† Electronic supplementary information (ESI) available. See DOI: 10.1039/c4ta03551h

composites, and these NGs showed an output voltage of 3.2 V and an output current of 67.5 nA.<sup>5</sup> However, detailed studies to determine the optimum amount of KN nanowires and to investigate the effect of process conditions on the output energy of KN NGs have not been carried out.<sup>5</sup> The KN ceramic has a cubic structure at temperatures higher than 435 °C, and it changes to a tetragonal structure at 225 °C. The orthorhombic structure is stable at temperatures between 225 and −10 °C but it changes to a rhombohedral structure at −10 °C. However, some previous studies have reported that KN nanowires having a tetragonal and a polymorphic phase boundary (PPB) structure, which contains both tetragonal and orthorhombic structures, are also formed at low temperatures.<sup>19,25</sup> Moreover, KN nanowires having a PPB structure show a large  $d_{33}$  value of 145.98 pm V<sup>−1</sup>.<sup>19</sup> Therefore, NGs synthesized using PPB KN nanowires are expected to show large output electrical energy. However, thus far, the existence of KN nanowires having tetragonal and PPB structures has not been explained, and NGs synthesized using KN nanowires having various structures have not been investigated. In this study, therefore, the presence of tetragonal and PPB KN nanowires was investigated; moreover, NGs consisting of various KN nanowires were synthesized and their output voltage and current were evaluated. Finally, the optimum amount of KN nanowires and their output energy for the NGs were also investigated.

## Experimental section

KN nanowires having tetragonal, PPB, and orthorhombic structures were synthesized by the hydrothermal method.<sup>19,25</sup> Varying amounts (0.1–0.8 g) of KN nanowires were mixed with 3.0 g of PDMS (Sylgard 184, Dow Corning), and the K–P mixture was coated on a Au-coated polyimide (PI) film at 2000 rpm (33<sup>−1</sup>) for 30 s. The thickness of the K–P composite layer was approximately 109 μm, and a 100 nm-thick Au electrode was formed on the 125 μm-thick PI film by DC sputtering. Another Au-coated PI (PI-Au) film with the same thickness was attached on top of the K–P composite/Au-PI layers, and the layers were baked at 70 °C for 12 h. The K–P composite was poled under an electric field of 5.0 kV mm<sup>−1</sup> for 1 h at RT. Finally, the PI-Au/K–P composite/Au-PI layers were attached on a 500 μm-thick polyethylene terephthalate (PET) substrate to synthesize piezoelectric NGs. The dimensions of the NGs synthesized in this study were 3.0 cm (L) × 3.0 cm (W) × 359.2 μm (T). A Fourier transform infrared spectrometer (FT-IR; Infinity Gold FT-IR series, Thermo Mattson, USA) was used to identify defects in the KN nanowires, and thermogravimetric analysis (TGA; DSC2010, TA Instrument, USA) was used to measure the weight loss in the nanowires. X-ray diffraction (XRD; Rigaku D/max-RC, Tokyo, Japan), scanning electron microscopy (SEM; Hitachi S-4300, Osaka, Japan), and field-emission transmission electron microscopy (FE-TEM; Tecnai F20, FEI, Netherlands) were used to investigate the structure and microstructure of the KN nanowires and NGs. The dielectric constant ( $\epsilon_r$ ) and dielectric loss ( $\tan \delta$ ) of the K–P composites were measured using an HP42894A impedance analyzer (Agilent, USA) at frequencies from 0.1 kHz to 100 kHz. Stress was applied on the NGs by using

a bending tester (ZBT-200, Zeetech, Korea), and the strain developed in the K–P composites was calculated using eqn (2) given in the ESI.† The open-circuit voltage and short-circuit current of the NGs were measured using a nano-voltage meter (Keithley 2182A: input impedance of >10 GΩ, delta mode, low noise measurements at high speeds, USA) and a pico-ampere meter (Keithley 6485 5-1/2 digit pico-ammeter: digital filter, up to 1000 readings per s, and 10 fA resolution, USA), respectively.

## Results and discussion

Fig. 1(a) shows the FT-IR spectra of the tetragonal, PPB, and orthorhombic KN nanowires. The FT-IR spectrum of the tetragonal KN nanowires shows a broad band at approximately 3500 cm<sup>−1</sup>; this band formed owing to the overlap of the O–H stretching vibrations of H<sub>2</sub>O and hydroxyl ions. However, this absorption was not observed in the spectra of the PPB and orthorhombic KN nanowires. Therefore, it is considered that the tetragonal KN nanowires contain more OH<sup>−</sup> and water molecules than the PPB and orthorhombic KN nanowires. The TGA curves of the tetragonal, PPB, and orthorhombic KN nanowires are shown in Fig. 1(b). The TGA curves of the PPB and orthorhombic KN nanowires show small weight losses of

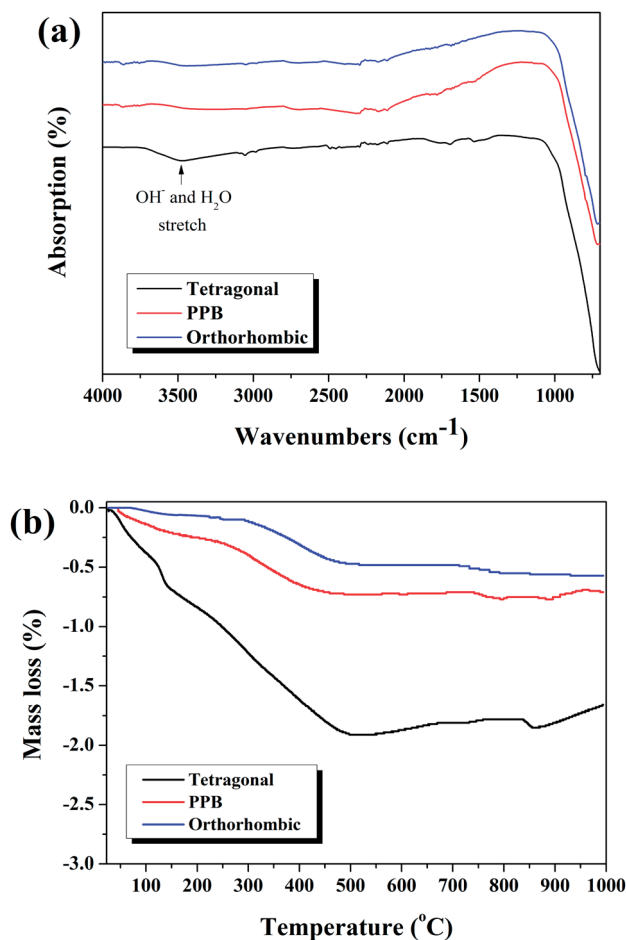


Fig. 1 (a) FT-IR spectra and (b) TGA curves of the tetragonal, PPB, and orthorhombic KN nanowires.

0.75% and 0.55%, respectively, up to 900 °C, indicating the presence of a small number of defects in these nanowires. For the tetragonal KN nanowires, however, the total weight loss up to 900 °C was relatively large, *i.e.*, 1.8%. Therefore, the tetragonal KN nanowires are considered to contain a large number of OH<sup>−</sup> and water molecules. This result coincides with that derived from the FT-IR spectra of the nanowires. Moreover, on the basis of TGA and FT-IR results, the formation of the tetragonal KN nanowires can be attributed to the presence of OH<sup>−</sup> and H<sub>2</sub>O defects. Similar results have been reported in previous studies.<sup>20,21</sup>

The TGA curves of the PPB and orthorhombic KN nanowires indicate two types of weight loss. The first type of weight loss occurred gradually over a wide temperature range from RT to 500 °C; the second type of weight loss occurred suddenly over a narrow temperature range from 300 °C to 400 °C. The gradual weight loss could be attributed to the desorption of surface-adsorbed hydroxyl groups, and the sudden weight loss could be attributed to the desorption of lattice hydroxyl groups. Similar TGA curves have been observed for hydrothermally synthesized orthorhombic KN nanorods and nanopowders.<sup>20,21</sup> Moreover, KTaO<sub>3</sub> powders and large-sized BaTiO<sub>3</sub> nanopowders (≥90 nm), which showed a small weight loss, exhibited similar TGA curves.<sup>26–28</sup> On the other hand, the tetragonal KN nanowires, which showed significant weight loss, exhibited a gradual weight loss, probably owing to the desorption of a large amount of surface-adsorbed hydroxyl groups.<sup>20</sup> Similar TGA curves have been obtained for small-sized BaTiO<sub>3</sub> nanopowders and KN nanopowders having a cubic or tetragonal structure, which showed a significant weight loss.<sup>20,29,30</sup> Therefore, it is considered that the amount of surface-adsorbed hydroxyl groups increases with an increase in the number of OH<sup>−</sup> defects.

The KN nanowires were expected to have an orthorhombic structure at RT; however, they exhibited a tetragonal structure, probably because of the presence of a large number of OH<sup>−</sup> ions and water molecules. In order to clarify the effect of these defects on the crystal structure of the KN nanowires, XRD patterns of the tetragonal, PPB, and orthorhombic KN nanowires were recorded after annealing them at 500 °C for 4 h, because most of the defects evaporate at around 500 °C.

Fig. 2(a) and (b) show the XRD peaks at 45° obtained *via* slow scanning, for the orthorhombic, PPB, and tetragonal KN nanowires before and after annealing at 500 °C for 4 h, respectively. These figures show that the PPB and tetragonal KN nanowires [Fig. 2(a)] changed into orthorhombic KN nanowires and that the peaks for the orthorhombic KN nanowires became sharp and narrow after the heat treatment at 500 °C [Fig. 2(b)]. These results confirm that the existence of tetragonal and PPB KN nanowires can be attributed to the presence of OH<sup>−</sup> and H<sub>2</sub>O defects. In order to investigate variations in the crystal structure of the KN nanowires, the tetragonal KN nanowires were annealed at various temperatures. Their XRD peaks at 45° were obtained *via* slow scanning and the results are shown in Fig. 2(c). The tetragonal structure of the KN nanowires started to change into the orthorhombic structure for specimens annealed at 200 °C; however, the structural variation was not significant for specimens annealed at 300 °C. Further, KN nanowires annealed at 400 °C showed the orthorhombic structure, indicating that the structural variation in these nanowires mostly occurred at temperatures between 300 and 400 °C. Furthermore, since the desorption of lattice hydroxyl groups occurred in the temperature range 300–400 °C, the structural change of the KN nanowires from tetragonal and orthorhombic could be closely related to this desorption.

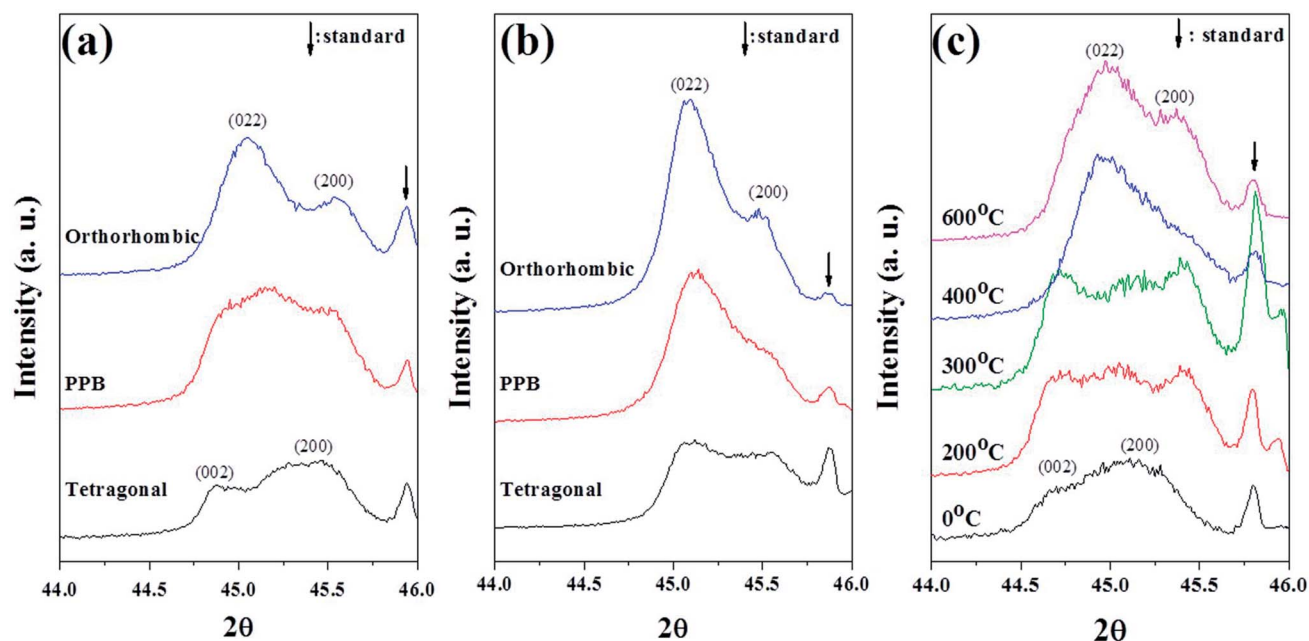


Fig. 2 XRD peaks at 45° obtained *via* slow scanning for the orthorhombic, PPB, and tetragonal KN nanowires (a) before and (b) after annealing at 500 °C for 4 h. (c) XRD peaks at 45° obtained *via* slow scanning for the tetragonal KN nanowires annealed at various temperatures.



In order to identify the crystal structure of the KN nanowires, Rietveld analysis was conducted on the XRD patterns of the nanowires. The lattice parameters for the tetragonal KN nanowires were  $a = 4.0046(2)$  Å and  $c = 4.0415(2)$  Å with the space group  $P4mm$  (Fig. S2 of the ESI†) and those for the orthorhombic KN nanowires were  $a = 3.9932(2)$  Å,  $b = 5.6978(6)$  Å, and  $c = 5.7027(6)$  Å with the space group  $Amm2$ . (Fig. S3 of the ESI†). On the other hand, the structure of the PPB KN nanowires can be explained by the presence of a mixture of a tetragonal phase with the space group  $P4mm$  and an orthorhombic phase with the space group  $Amm2$ . The refined lattice parameters were  $a = 4.0074(1)$  Å and  $c = 4.0401(3)$  Å for the tetragonal phase and  $a = 3.9875(3)$  Å,  $b = 5.7039(9)$  Å, and  $c = 5.7120(9)$  Å for the orthorhombic phase (Fig. S4 of the ESI†).

TEM analysis was also conducted to confirm the presence of the three crystal structures of the KN nanowires, as shown in Fig. 3(a)–(c). The selected area diffraction (SAD) patterns and the high-resolution TEM (HRTEM) images of the KN nanowires show that the KN nanowires have three different crystal structures. The tetragonal KN nanowires have a tapered shape and the orthorhombic and PPB KN nanowires have a rectangular shape because they were synthesized at higher temperatures or for a longer period of time as compared with the tetragonal KN nanowires. The growth direction of all the KN nanowires was  $[100]$ .<sup>19</sup> Therefore, on the basis of the XRD and TEM analysis, it can be suggested that the tetragonal, orthorhombic, and PPB KN nanowires were well synthesized with good crystalline quality.

The tetragonal, PPB, and orthorhombic KN nanowires were mixed with PDMS, thereby forming K–P composites. Piezoelectric NGs were then synthesized using these composites.

Fig. 4 shows a cross-sectional SEM image of an NG. It can be observed that the 109 µm-thick K–P composite layer was well formed, with a sharp and continuous interface between the K–P composite and the Au-coated PI film. The Au electrode is not shown in Fig. 4(a) because of its small thickness. The inset of Fig. 4 shows a magnified SEM image of the K–P composite. The white spots shown in this figure represent KN nanowires; it can be observed that they were well dispersed in PDMS.

Fig. 5(a) shows the  $\epsilon_r$  and  $\tan \delta$  of pure PDMS and the K–P composite containing 0.3 g of KN nanowires having various structures. The  $\epsilon_r$  and  $\tan \delta$  values of PDMS were 2.2 and 0.025%, respectively, at 100 kHz; variations in these values as a function of the measuring frequency were negligible. The K–P composite containing the orthorhombic KN nanowires had a relatively low  $\epsilon_r$  value of 2.8 at 100 kHz. The K–P composite containing the tetragonal KN nanowires showed a slightly higher  $\epsilon_r$  value of 3.7 at 100 kHz. On the other hand, the K–P composite containing the PPB KN nanowires showed a high  $\epsilon_r$  value of 5.6 at 100 kHz. The  $\tan \delta$  value of the K–P composite containing the tetragonal KN nanowires was larger than that of the K–P composites containing the PPB or orthorhombic KN nanowires at low frequencies. This difference could be due to the presence of a large number of  $\text{OH}^-$  and  $\text{H}_2\text{O}$  defects in the tetragonal KN nanowires. However, all K–P composites showed a low  $\tan \delta$  value of approximately 0.3% at 100 kHz. The  $\epsilon_r$  and  $\tan \delta$  values of the K–P composite containing 0.7 g of KN nanowires were also measured, and the results are shown in Fig. 5(b).

The  $\epsilon_r$  values of all K–P composites increased with an increase in the amount of KN nanowires. In particular, the K–P composite containing the PPB KN nanowires showed the highest  $\epsilon_r$  value of 9.2 but a low  $\tan \delta$  value of 0.5% at 100 kHz. It is worth mentioning here that the  $\epsilon_r$  value of the K–P composite containing the tetragonal KN nanowires was larger than that of the K–P composite containing the orthorhombic KN nanowires. The larger  $\epsilon_r$  value of the K–P composite containing the tetragonal KN nanowires could be attributed to the presence of a large number of metal vacancies in the tetragonal KN nanowires due to the presence of  $\text{OH}^-$  defects at  $\text{O}^{2-}$  sites.

Fig. 6(a)–(c) show the open-circuit voltage of NGs containing 0.7 g of KN nanowires, as measured along the forward direction with a strain and strain rate of 2.1% and  $2.2\% \text{ s}^{-1}$ , respectively. The output voltage of the NG containing the orthorhombic KN

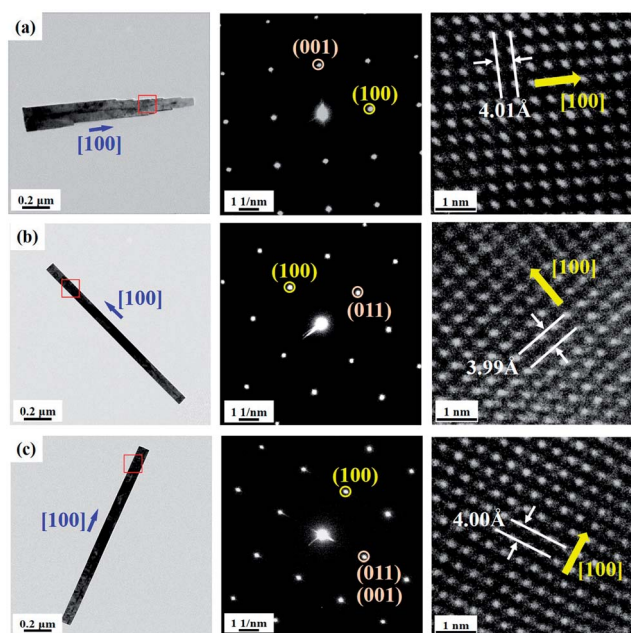


Fig. 3 Bright-field images, SAD patterns, and HRTEM images of the KN nanowires with (a) tetragonal, (b) orthorhombic, and (c) PPB KN nanowires.

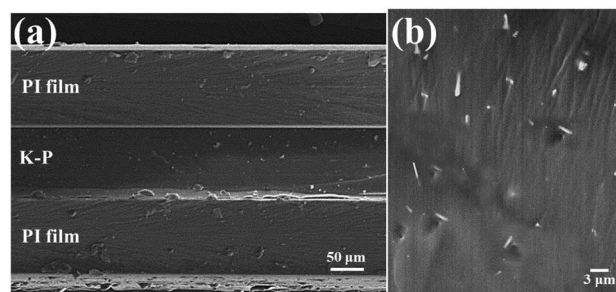


Fig. 4 (a) Cross-sectional SEM image of an NG and (b) magnified SEM image of the K–P composite (white spots denote KN nanowires).

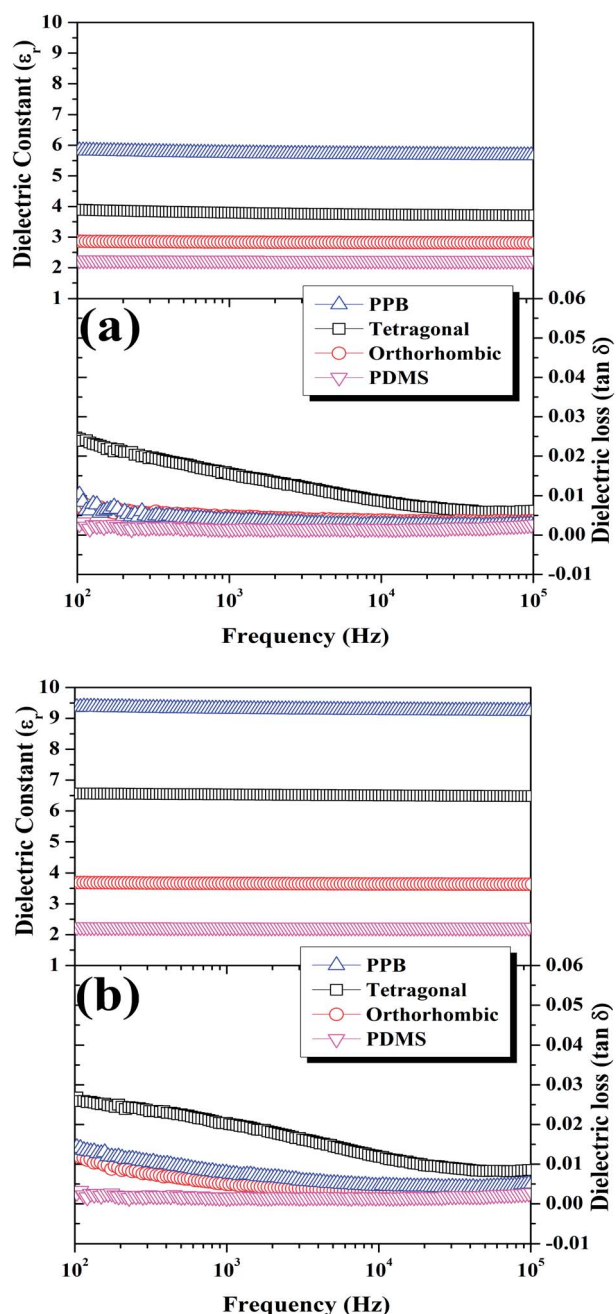


Fig. 5 Dielectric constant ( $\epsilon'$ ) and dielectric loss ( $\tan \delta$ ) of KN-PDMS composites containing (a) 0.3 g of KN nanowires and (b) 0.7 g of KN nanowires having various structures.

nanowires was measured to be 6.0 V. Further, the NG containing the tetragonal KN nanowires showed a larger output voltage of 9.1 V. Finally, the NG containing the PPB KN nanowires showed the largest output voltage of 10.5 V.

The short-circuit current of NGs containing 0.7 g of KN nanowires was also measured, and the results are shown in Fig. 7(a)–(c). The NG containing the orthorhombic KN nanowires exhibited a small short-circuit current of 0.55  $\mu\text{A}$ . Further, the NG containing the tetragonal KN nanowires showed a larger short-circuit current of 0.99  $\mu\text{A}$ . Finally, the NG containing the

PPB KN nanowires exhibited the largest short-circuit current of 1.3  $\mu\text{A}$ . Similar results were obtained when the output voltage and current were measured along the reverse direction, as shown in Fig. S5(a) and (b) of the ESI.† Five NGs for each structure of KN nanowires (15 NGs total) were synthesized, and they exhibited a similar output voltage and output current, as shown in Fig. 6 and 7. In addition, NGs containing 0.3 g of KN nanowires showed similar variation of the output electrical energy with respect to the structure of the KN nanowires (see Fig. S6 and S7 of the ESI.†). Therefore, it can be concluded that the variations of the output electrical energy shown in Fig. 6 and 7 are reliable and that the NG containing the PPB KN nanowires exhibited the maximum output electrical energy. The output power and the energy conversion efficiency of each NG were obtained using external loads, as shown in the ESI.† The NG containing the PPB KN nanowires exhibited the maximum output power and energy conversion efficiency, which were 4.5  $\mu\text{W}$  and 0.9%, respectively, for an external load of 1.0  $\text{M}\Omega$ .

Since the output voltage and current of the PDMS NG were very low [Fig. S12(a) and (b) of the ESI.†], it can be concluded that the output voltage and current of the NGs originated from the KN nanowires.

According to a previous study, PPB KN nanowires showed a larger  $d_{33}$  value (146  $\text{pm V}^{-1}$ ) than the tetragonal (137  $\text{pm V}^{-1}$ ) and orthorhombic (104.5  $\text{pm V}^{-1}$ ) KN nanowires.<sup>19</sup> In addition, schematic diagrams, which show that the PPB KN nanowires had improved piezoelectric properties, are shown in Fig. S13(a)–(c) and S14(a)–(d) of the ESI.† Therefore, the largest output electric energy obtained from the NG containing PPB nanowires can be attributed to its large  $d_{33}$  value; this is because the output energy density of a piezoelectric nanogenerator is proportional to  $d_{33}^2$ .<sup>12–14</sup> Moreover, the output voltage of 10.5 V and the output current of 1.3  $\mu\text{A}$  are among the highest reported values for NGs synthesized using PDMS-nanowires composites.<sup>1,4–9</sup>

Fig. 8(a) and (b) show the open-circuit output voltage and short-circuit output current of NGs containing various amounts of the PPB KN nanowires. The voltage and current were measured along the forward direction under a strain and strain rate of 2.1% and 2.2%  $\text{s}^{-1}$ , respectively. The voltage and current of the NG containing a small amount of KN nanowires ( $\leq 0.2$  g) were very small and increased with an increase in the amount of nanowires. The NG containing 0.7 g of KN nanowires showed the maximum output voltage and current. However, for the NG containing 0.8 g of KN nanowires, the Au electrode was easily separated from the K–P composite during the poling process because the adhesive strength of PDMS decreased considerably when 0.8 g of KN nanowires was mixed with PDMS. Similar results were obtained when the output voltage and current were measured along the reverse direction, as shown in Fig. S15(a) and (b) of the ESI.† Therefore, it can be suggested that 3.0 g of PDMS can contain 0.7 g of KN nanowires, corresponding to 23.0 wt% of KN nanowires. The voltage and current for the NG containing 0.7 g of PPB KN nanowires were measured along the forward direction at a constant strain rate of 2.2%  $\text{s}^{-1}$  and various strains, and the results are shown in Fig. S16(a) and (b) of the ESI.† They were also measured at a constant strain of 2.1% and various strain rates, and the results are shown in

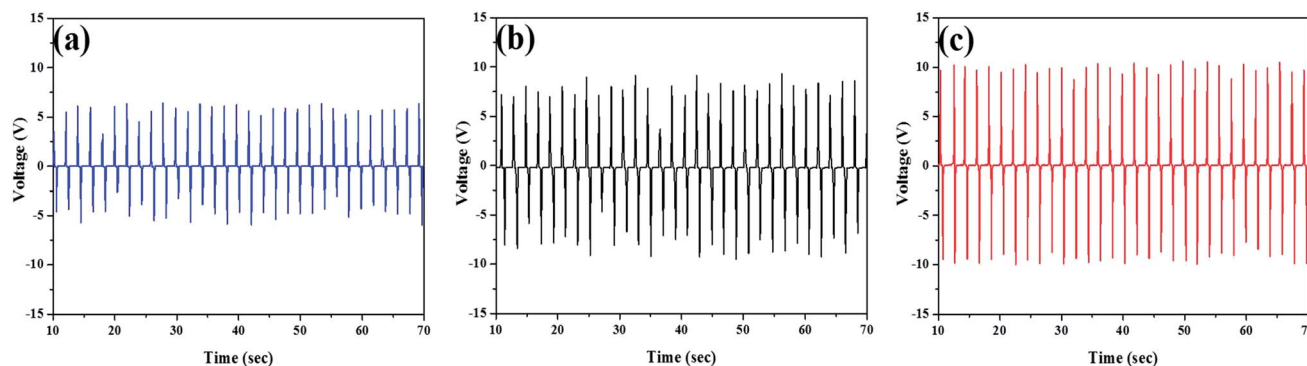


Fig. 6 Open-circuit voltage of NGs containing 0.7 g of KN nanowires having various structures: (a) orthorhombic, (b) tetragonal, and (c) PPB.

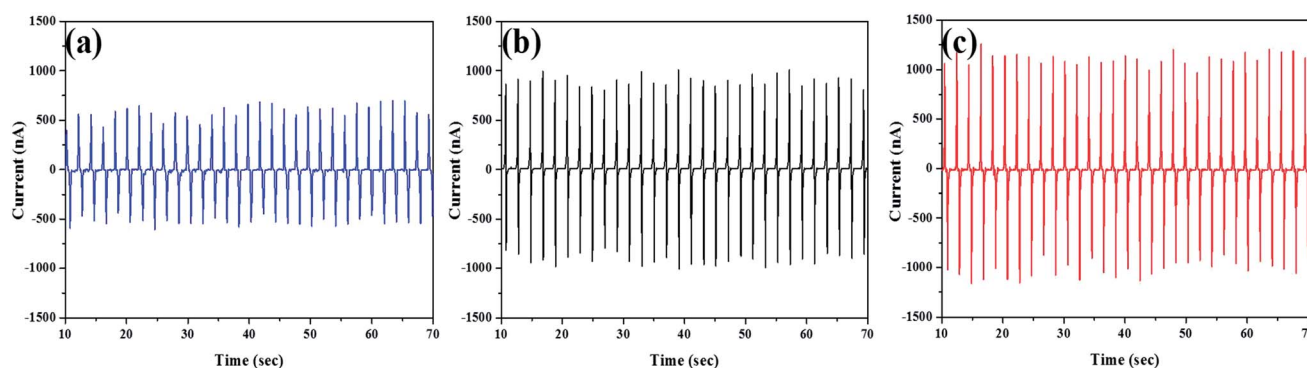


Fig. 7 Short-circuit current of NGs containing 0.7 g of KN nanowires having various structures: (a) orthorhombic, (b) tetragonal, and (c) PPB.

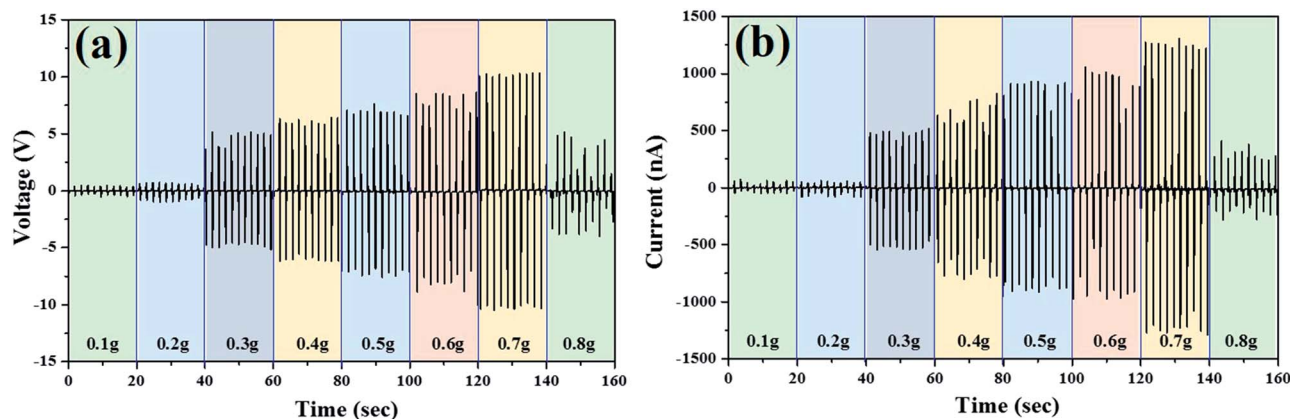


Fig. 8 (a) Open-circuit output voltage and (b) short-circuit output current of NGs containing various amounts of PPB KN nanowires. The voltage and current were measured along the forward direction at a strain and strain rate of 2.1% and  $2.2\% \text{ s}^{-1}$ , respectively.

Fig. S17(a) and (b) of the ESI.† The voltage and current increased with increasing strain and strain rate, and a maximum voltage of 10.5 V and a maximum current of  $1.3 \mu\text{A}$  were obtained when the strain and strain rate were 2.1% and  $2.2\% \text{ s}^{-1}$ , respectively.

## Conclusions

KN nanowires were expected to have an orthorhombic structure at RT. However, KN nanowires having tetragonal and PPB

structures were also present at RT, when they contained a large number of  $\text{OH}^-$  and  $\text{H}_2\text{O}$  defects. The PPB and tetragonal structures of the KN nanowires changed to an orthorhombic structure at temperatures between  $300^\circ\text{C}$  and  $400^\circ\text{C}$  owing to the desorption of the lattice hydroxyl groups. The structure of the PPB KN nanowires was explained by the mixture of tetragonal ( $P4mm$ ) and orthorhombic ( $Amm2$ ) structures. The K-P composites synthesized using PPB KN nanowires exhibited the largest  $\epsilon_r$  value among the K-P composites synthesized using tetragonal, orthorhombic, and PPB KN nanowires. In particular,



the K-P composite containing 0.7 g of PPB KN nanowires showed a high  $\epsilon_r$  and a low  $\tan \delta$  value of 9.2 and 0.5%, respectively. The NG containing PPB KN nanowires exhibited a larger output voltage and current than those containing tetragonal or orthorhombic KN nanowires. This difference could be due to the fact that the PPB nanowires show a larger  $d_{33}$  value than the tetragonal and orthorhombic KN nanowires. The NG containing 0.7 g of PPB KN nanowires showed a maximum output voltage of 10.5 V and a maximum output current of 1.3  $\mu\text{A}$  when they were measured under a strain and strain rate of 2.1% and 2.2%  $\text{s}^{-1}$ , respectively. These output voltage and current values are among the highest reported for NGs synthesized using PDMS-nanowire composites. Therefore, NG containing PPB KN nanowires are good candidates for power sources in microelectronics.

## Acknowledgements

This work was supported by the BK21 plus program through the National Research Foundation (NRF) funded by the Ministry of Education of Korea and the 'Development of Nano-carbons for energy conversion and storage' funded by the Korea Institute of Energy Research (KIER, Korea).

## Notes and references

- 1 X. Chen, S. Xu, N. Yao and Y. Shi, *Nano Lett.*, 2010, **10**, 2133.
- 2 K.-I. Park, S. Xu, Y. Liu, G.-T. Hwang, S. J. L. Kang, Z. L. Wang and K. J. Lee, *Nano Lett.*, 2010, **10**, 4939.
- 3 K.-Y. Lee, B. Kumar, J.-S. Seo, K.-H. Kim, J. I. Sohn, S. N. Cha, D. Choi, Z. L. Wang and S.-W. Kim, *Nano Lett.*, 2012, **12**, 1959.
- 4 K.-I. Park, M. Lee, Y. Liu, S. Moon, G.-T. Hwang, G. Zhu, J.-E. Kim, S.-O. Kim, D.-K. Kim, Z. L. Wang and K.-J. Lee, *Adv. Mater.*, 2012, **24**, 2999.
- 5 J.-H. Jung, C.-Y. Chen, B.-K. Yun, N. Lee, Y. Zhou, W. Jo, L.-J. Chou and Z. L. Wang, *Nanotechnology*, 2012, **23**, 375401.
- 6 Z.-H. Lin, Y. Yang, J. M. Wu, Y. Liu, F. Zhang and Z. L. Wang, *J. Phys. Chem. Lett.*, 2012, **3**, 3599.
- 7 J.-H. Jung, M.-B. Lee, J.-I. Hong, Y. Ding, C.-Y. Chen, L.-J. Chou and Z. L. Wang, *ACS Nano*, 2011, **5**, 10041.
- 8 S. Xu, Y. W. Yeh, G. Poirier, M. C. McAlpine, R. A. Register and N. Yao, *Nano Lett.*, 2013, **13**, 2393.
- 9 C.-K. Jeong, K.-I. Park, J.-H. Ryu, G.-T. Hwang and K.-J. Lee, *Adv. Funct. Mater.*, 2014, **24**, 2620.
- 10 Z. L. Wang and W. Wu, *Angew. Chem., Int. Ed.*, 2012, **51**, 11700.
- 11 D. Karanth and H. Fu, *Phys. Rev. B: Condens. Matter Mater. Phys.*, 2005, **72**, 064116.
- 12 R. A. Islam and S. Priya, *J. Am. Ceram. Soc.*, 2006, **88**, 3147.
- 13 R. A. Islam and S. Priya, *Appl. Phys. Lett.*, 2006, **88**, 032903.
- 14 Z. Wang, J. Hu, A. P. Suryavanshi, K. Yum and M. F. Yu, *Nano Lett.*, 2007, **7**, 2966.
- 15 C. F. Carl, *J. Chem. Phys.*, 1962, **36**, 798.
- 16 L. A. Reznitchenko, A. V. Turik, E. M. Kuznetsova and V. P. Sakhnenko, *J. Phys.: Condens. Matter*, 2001, **13**, 3875.
- 17 K. Nakamura, T. Tokiwa and Y. Kawamura, *J. Appl. Phys.*, 2002, **91**, 9272.
- 18 S. Wada, A. Seike and T. Tsurumi, *Jpn. J. Appl. Phys.*, 2001, **40**, 5690.
- 19 M.-R. Joung, I.-T. Seo, J.-S. Kim, H. Xu, G. Han, M.-G. Kang, C.-Y. Kang, S.-J. Yoon and S. Nahm, *Acta Mater.*, 2013, **61**, 3703.
- 20 N. Kumada, T. Kyoda, Y. Yonesaki, T. Takei and N. Kinomura, *Mater. Res. Bull.*, 2007, **42**, 1856.
- 21 B.-K. Yun, Y.-S. Koo, J.-H. Jung, M. Song and S. Yoon, *Mater. Chem. Phys.*, 2011, **129**, 1071.
- 22 B.-K. Yun, Y.-S. Koo, J.-H. Jung, M. Song and S. Yoon, *Phys. B*, 2010, **405**, 4866.
- 23 G. Wang, Y. Yu, T. Grande and M.-A. Einarsrud, *J. Nanosci. Nanotechnol.*, 2009, **9**, 1465.
- 24 G. Wang, S. M. Selbach, Y. Yu, X. Zhang, T. Grande and M.-A. Einarsrud, *CrystEngComm*, 2009, **11**, 1958.
- 25 M.-R. Joung, H. Xu, J.-S. Kim, I.-T. Seo, S. Nahm, J.-Y. Kang and S.-J. Yoon, *J. Appl. Phys.*, 2012, **111**, 114314.
- 26 T. Noma, S. Wada, M. Yano and T. Suzuki, *J. Appl. Phys.*, 1996, **80**, 5223.
- 27 S. Wada, T. Suzuki and T. Noma, *Jpn. J. Appl. Phys.*, 1995, **34**, 5368.
- 28 G. K. L. Goh, S. M. Haile, C. G. Levi and F. F. Lange, *J. Mater. Res.*, 2002, **17**, 3168.
- 29 S. Wada, T. Suzuki and T. Nama, *J. Ceram. Soc. Jpn.*, 1995, **103**, 1220.
- 30 S. Wada, T. Suzuki and T. Noma, *J. Ceram. Soc. Jpn.*, 1996, **104**, 383.